The synthesis and characterization of PbS/ PVA-Mg-Al-LDH nanocomposite film

Kh. A. Ibrahimova[a,*], A. A. Azizov[a], O. O. Balayeva[a], R. M. Alosmanov[a],
R. M. Aghayeva[b], M. H. Abbasov[c]
[a]*Department of Chemistry, Baku State University, Z.Khalilov st., 23, AZ-1148 Baku, Azerbaijan*
[b]*Department of Chemistry and Biology, Azerbaijan State Pedagogical University, AZ-1000 Baku 68, Uzeyir Hajibeyli str., Baku, Azerbaijan*
[c]*Department of Chemistry,* Institute of Catalysis and Inorganic chemistry of the Azerbaijan National Academy of Sciences*, H.Javid Ave., 113, AZ-1143 Baku, Azerbaijan*

This paper described the synthesis of lead(II)sulfide (PbS) based nanocomposite on polyvinyl alcohol/magnesium-aluminum–layered double hydroxide (PVA/Mg-Al-LDH) composite film by a successive ionic layer adsorption and reaction (SILAR) method. To characterize the prepared sample was carried out using X-ray powder diffraction analysis (XRD), Ultraviolet-visible (UV-Vis) spectroscope, Scanning electron microscope (SEM), Energy-dispersive X-ray (EDX) spectroscope, and Fourier transform infrared (FT-IR) spectroscope was used. The optical absorption study confirmed when the PbS nanoparticles are dispersed in the PVA polymer matrix, they can well fit the interstitial spaces between the polymer chains and thus an increase in the optical conductivity.

(Received June 2, 2022; Accepted November 1, 2022)

Keywords: Layered double hydroxide, Polymer nanocomposite, Film, Structural analysis, Optical properties

1. Introduction

Nanostructured materials have attracted extraordinary research interest owing to their fundamental importance for addressing some basic issues of the quantum confinement effect [1].

Polymer nanocomposites is a class of material because of various unique properties such as improved mechanical properties, gas barrier properties, reduced flammability, increased heat distortion temperature, reduced solvent uptake, and lower flammability [2].

Recently, PVA-based nanocomposites have been composed to improve PVA properties and further explore its applications by the solution casting method [3]. Polyvinyl alcohol (PVA) is a water-soluble polymer frequently used as a colloid stabilizer [4]. The introduction of stabilizers influences the chemical properties as well as the physical properties of semiconductor materials, from stability, solubility, and light emission [5]. It has a semicrystalline nature that arises from the role of the OH group and the hydrogen bonds [3, 5]. LDH has known as a new class of the most promising layered materials incorporated into polymer matrices as reinforcing filler[4]. When LDH being included in polymer matrices and properties of the prepared nanocomposites can be improved the thermal stability, flame retardancy, mechanical, and rheological properties[2]. The usage of nanoparticles as a flier of polymeric materials relates to the strong current interest in the development and application of new materials [6].

Among all nanoparticles lead sulfide (PbS) proved to be an important semiconductor, that attracted much attention, due to attractive non-linear optical properties, and a typical narrow direct allowed band gap (0.41 eV at room temperature) [7-9]. The PbS nanoparticles have vital applications in a nonlinear optical device like absorbers in solar cells, optical information storage, infrared detector, gas sensor, optical amplification, and optical switches, due to the exceptional third-order non-linear optical properties [10-14].

---

[*] Corresponding author: khazangul.ibrahimova1994@mail.ru

https://doi.org/10.15251/CL.2022.1911.761

In this context, we report the synthesis of PbS based nanocomposite on PVA/Mg-Al-LDH composite film by a successive ionic layer adsorption and reaction (SILAR) method. The aim of the work is to introduce a new class of polymer-filled nanoparticles with a simple method of preparation and investigated structure through experimental methods. The synthesized PbS containing nanocomposites might be used in the fabrication of novel optical, solar cell, and electronic devices. The reaction was carried out at room temperature. The results obtained from X-ray, SEM, EDX, UV-Vis, and FTIR spectroscopy experiments are reported.

2. Experimental section

2.1. Materials and instrumentation

All chemicals magnesium hydroxide [$Mg(OH)_2$], aluminum hydroxide [$Al(OH)_3$], polyvinyl alcohol (PVA), lead(II)acetate trihydrate [$Pb(CH_3COO)_2{\cdot}3H_2O$] and sodium sulfide nonahydrate [$Na_2S{\cdot}9H_2O$] were of analytical grade. All the experiments were used distilled water.

2.2. The synthesis of PVA/Mg-Al-LDH thin film

Bath type ultrasonicator (VCX500) was used for the synthesis of PVA/Mg-Al-LDH composite film. For the prepared film, 4 g of PVA was dissolved in 40 ml distilled water. 0.3 g of Mg-Al-LDH dry powder was added into 10 ml 10% PVA solution and ultrasonically stirred for 10 min at room temperature. The solution was dried at room temperature.

2.3. The synthesis of PbS/PVA-Mg-Al-LDH nanocomposite film

The preparation of PbS nanocomposite based on PVA/Mg-Al-LDH compositefilm was carried out by a successive ionic layer adsorption and reaction (SILAR) method. For the synthesise of PbS/PVA-Mg-Al-LDH nanocomposite film, 50 ml 0.1 M $Pb(CH_3COO)_2{\cdot}3H_2O$ solution was used as the first cation source and 50 ml 0.1 M $Na_2S{\cdot}9H_2O$ solution was used anion source. 0.4 g PVA/Mg-Al-LDH composite film was immersed into 50 ml 0.1 M $Pb(CH_3COO)_2{\cdot}3H_2O$ solution for 1 min and washed with distilled water. The sulfirizing processes was carried out with 50 ml 0.1 M $Na_2S{\cdot}9H_2O$ solution for 1 min. Sample was washed with distilled water and this process was carried out in 5 and 10 cycles and air-dried.

$$\mathrm{Pb}(CH_3\mathrm{COO})_2 + \mathrm{Na_2S} \rightarrow \mathrm{PbS} \downarrow + 2CH_3COONa \quad (1)$$

2.4. Characterization

Powder X-ray diffractometer (XRD) (Bruker D2 Phaser) in CuKα radiation ($\lambda = 0.1541$ nm) was used in the angular range $2\theta = 10$–$80°$ to characterize the structural properties of the samples.

Optical characterization was carried out by Specord 210 plus UV–Vis spectrometer.

JEOL ISM-7600F Scanning electron microscope (SEM) and X-max 50 energy dispersive X-ray spectrometer (EDX) were used to characterize the surface morphology and chemical composition of the products.

Fourier-transform infrared spectroscopy (FT-IR) spectra were recorded within 500–4000 cm^{-1} region on a NICOLET IS10 FTIR spectrometer.

3. Results and discussion

3.1. Structural properties

XRD pattern of PVA/Mg-Al-LDH composite film prepared by the sonochemical method are shown in [Figure 1 (curve (1))].

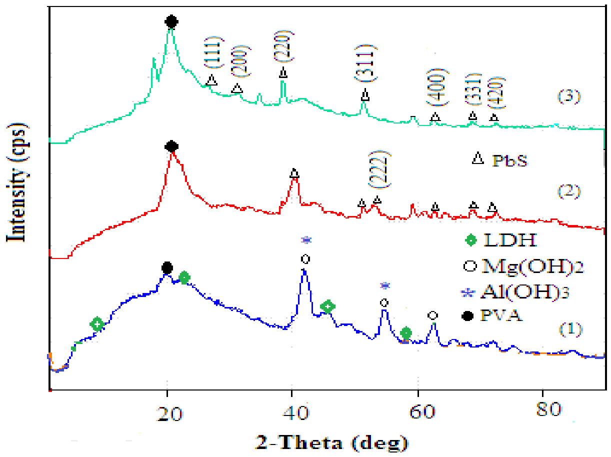

Fig. 1. XRD pattern of (1) PVA/Mg-Al-LDH composite film;PbS/PVA-Mg-Al-LDH nanocomposite films synthesized at (2) 5 cycle and (3) 10 cycles.

PVA is a crystalline polymer and the diffraction peak at 2θ=19.98° correspond to that of the PVA monoclinic crystalline phase [15].

The average size of nanoparticles has been calculated using the Debye–Scherrer equation [16, 17].

$$D = \frac{\alpha\lambda}{\beta\cos\theta} \tag{2}$$

where D is the particle diameter, α is the Scherrer constant (0.9), λ is the X-ray wavelength (0.15418 nm), β is the full width of half maximum (FWHM), and θ is the Bragg's angle.

The XRD patterns of synthesized powders for PbS nanoparticles prepared based on polyvinyl alcohol composite film are shown in [Figure 1 (curve (2), (3))]. It shows several diffraction peaks at 2θ values of 26.5°, 31.26°, 42.58°, 51.3°, 53.5°, 62.53°, 68.81°, and 71.13° which correspond to the Miller index of the reflecting planes for (111), (200), (220), (311), (222), (400), (331), and (420). All the diffraction peaks in the spectra are analogous to the literature pattern of face-centered cubic phase PbS powder (JCPDS file no: 5-592), confirming the formation of PbS nanoparticles [18].The XRD pattern of the PbS particles in the polymer matrix shows broadening of the peaks in comparison to bulk PbS [19], which indicates that as-synthesized PbS thin film is nanocrystalline in the polymer PVA matrix. The PVA was used as an organic capping agent to control the growth of the PbS nanocrystal. The stabilization takes place via the formation of coordination bond between the lone pair of electrons of O^{2-} on PVA and vacant d orbital of Pb^{2+} in the PbS [20]. The intense and sharp diffraction peaks suggest that the as-obtained products are well crystallized. The intensity of the diffraction peak of the synthesized samples at 10 cycles is higher than at 5 cycles [Figure 1 (curve (3), (2))] which belongs to PbS nanoparticles. We observed that the intensity of the crystallization process increases with increasing cycle numbers. The average size of PbS nanoparticles was determined 4.08 nm and 1.33 nm.

3.2. Optical studies

The UV–Vis absorption spectra were used to characterize the electronic properties of the synthesized materials. Figure 2 shows the UV–Vis absorbance spectra of synthesized PbS nanocomposite based on PVA/Mg-Al-LDH composite film by the SILAR method. Mg-Al-LDH exhibited a quite low absorbance in the range of 200–800 nm [Figure 2 (curve (1))]. As shown in [Figure 2 (curve (2))], the absorption threshold of PVA/Mg-Al-LDH composite was about 350 nm. The absorption of light for a material occurs by the transfer of electrons from the valence band to the conduction band [21].

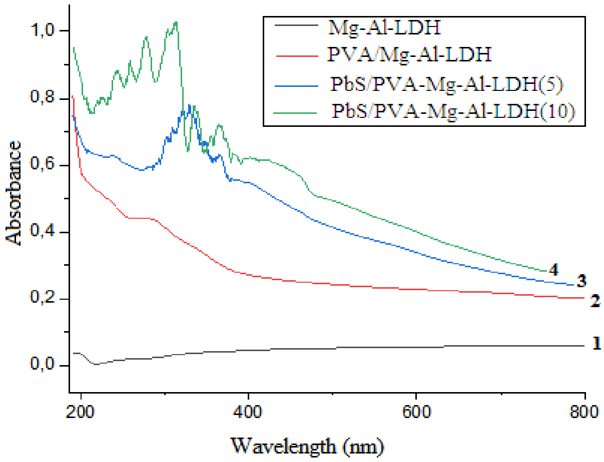

Fig. 2. UV-Vis absorption spectra of 1) Mg-Al-LDH; 2) PVA/Mg-Al-LDH composite film; 3) PbS/PVA-Mg-Al-LDH synthesized at 5 cycle; 4) PbS/PVA-Mg-Al-LDH synthesized at 10 cycle.

The optical absorption spectra analysis in solid material provides essential information about the band structure and the energy band gap in the materials [20, 21]. Compared with the PVA/Mg-Al-LDH composite, a shift in the absorption edge of the composites containing PbS can be observed, indicating the higher visible light response [Figure 2 (curve 3,4)]. The polymer was used as a stabilizer to control the optical properties of the PbS solution.When the PbS nanoparticles dispersed in PVA polymer matrix, they can well fit the interstitial spaces between the polymer chains and forms a segregated network [22], and thus an increase in the optical conductivity.

Patel et al., [23] found that PbS nanoparticles stabilized with PVA, exhibit a distinct band gap absorption and showed that the stabilized PbS with PVA, presents three distinct absorption peaks (290, 390, and 581 nm) corresponding to the electronic transitions. PVA capped PbS nanoparticles exhibit good optical properties due to the formation of smaller size particles [24]. When the size of a particle, in any dimension, is smaller than the Bohr exciton radius, which is characteristic of the material and defines the minimum distance between the charge carriers, the quantum confinement effects become observable [25]. Band gaps of semiconductors are also highly dependent on the morphology of the particles [23].

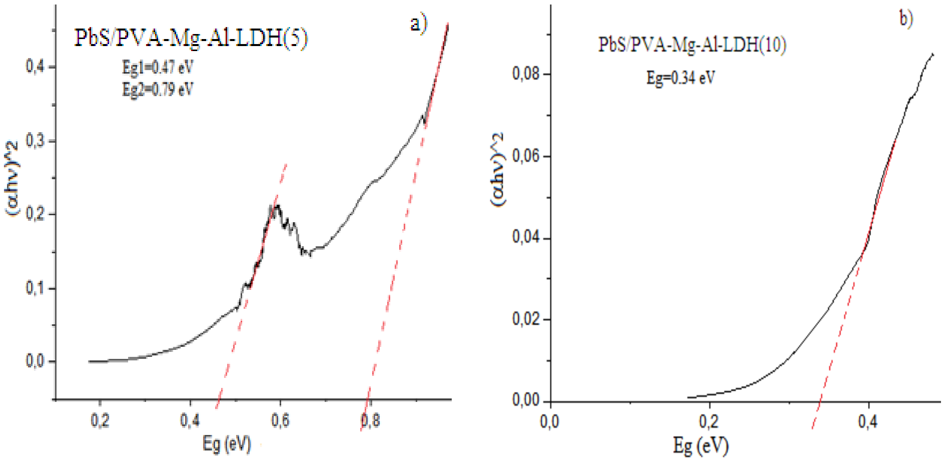

Fig. 3. UV-Vis calculated band gap of a) PbS/PVA-Mg-Al-LDH synthesized at 5 cycle; b) PbS/PVA-Mg-Al-LDH synthesized at 10 cycle.

For crystalline semiconductors, their optical band gaps could be calculated from the absorption spectra using the equation as follows [26].

$$\alpha h\nu = A(h\nu - E_g)^{n/2} \tag{3}$$

where α, ν, A, and E_g were the absorption coefficient, light frequency, the proportionality constant, and the optical band gap, respectively. n depended on the characteristics of transition in a semiconductor, and n=1 was confirmed here by the method mentioned in the literature [27].

The optical band gap of PbS nanoparticles is calculated as 0.47 eV and 0.34 eV [Figure 3 (a),(b)]. Bulk PbS has a direct gap at 0.41 e V at 300 K [28]. In narrow gap semiconductors, the large exciton radius and the strong screening can give small exciton binding energy and the absence of excitonic structures in the absorption edges [29]. As the semiconductor particle size decreases, in principle, the band gap can move to different points of the Brillouin zone due to the differences in effective masses of various bands [30].

3.3. Morfological analyses by SEM

In order to investigate the morphology of the composites and the distribution of PbS on the PVA/Mg-Al-LDH matrix, SEM microphotographs of the synthesized nanocrystals were shown in [Figure 4 (a), (b), (c)].

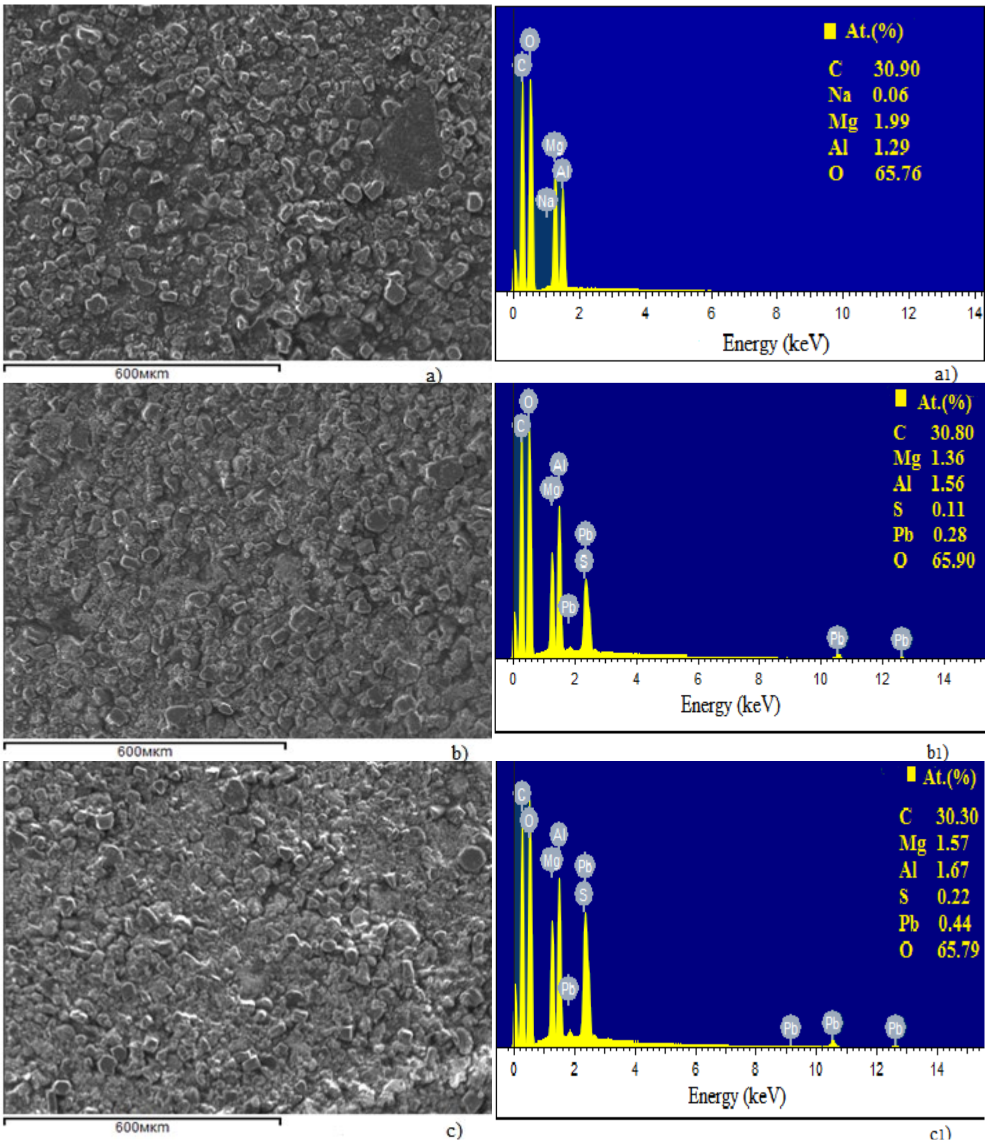

Fig. 4. SEM images (a), (b), (c) and EDX spectrum (a1), (b1), (c1) of PVA/Mg-Al-LDH; PbS/PVA-Mg-Al-LDH(5); PbS/PVA-Mg-Al-LDH(10) nanocomposites.

The SEM micrographs obtained clearly show that these plate-like particles are composed of hexagonally shaped nanoparticles that are characteristic of LDH structures [31]. We observed large and lumpy particles in the photo.The surface morphology of the synthesized polymer composite sample exhibits agglomeration [32] of fine particles in several microns, though the size of primary particles is in nanoscale. Figure 4 shown SEM images of the sample synthesized in 5 cycles (b) and 10 cycles (c). We observed that the particles are distributed across the polymer composite surface, and the deposited films are composed of regularly shaped crystallites in the two images.

The SEM-EDS analysis result showed clearly the presences of C (carbon), Mg (magnesium), Al (aluminum), S (sulfur), Pb (lead), and O (oxygen) in the PbS/PVA-Mg-Al-LDH composite [Figure 4.(b1),(c1). However, it shows that the Pb/S atomic ratio equal to 2.5 and 2 for (5) cycle and (10) cycle in the surface of the polymer composite material.

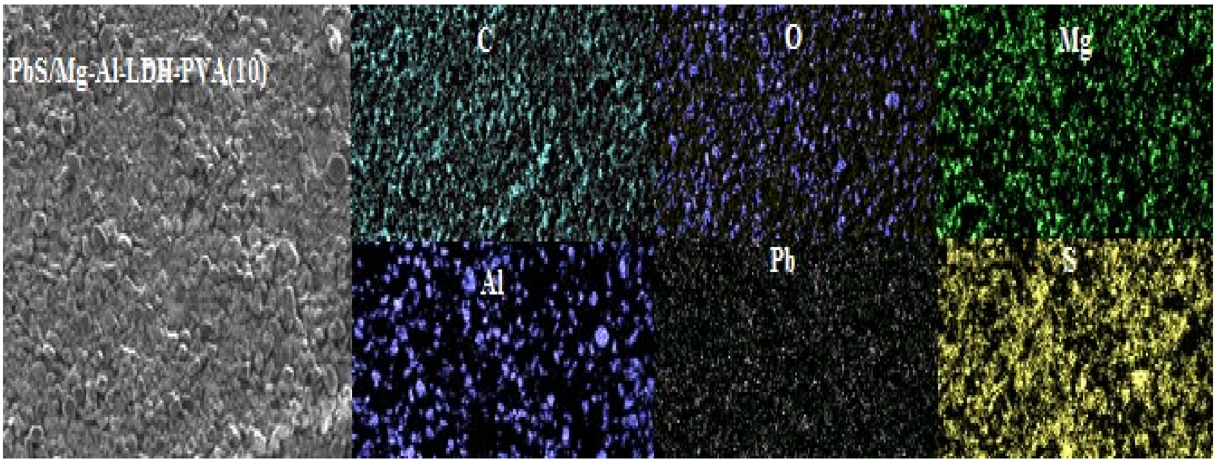

Fig. 5. SEM-Mapping analysis chart of PbS/PVA-Mg-Al-LDH(10) nanocomposite film.

Figure 5 shows an SEM-Mapping analysis of the nanocomposite surface that is distributed with C, Mg, Al, S, Pb, and O elements.

3.4. FT-IR spectroscopy study

Fourier transform infrared (FTIR) spectroscopy has been proven to be a technique to study the internal structure of polymeric materials and the intermolecular interaction between the polymeric material and filler. The synthesized samples were characterized by recording their FT-IR spectra in the range of 500-4000 cm^{-1} [Figure 6 (a;b;c)]. The spectra exhibited characteristic bands of stretching and bending vibrations of the functional groups formed in the prepared films.

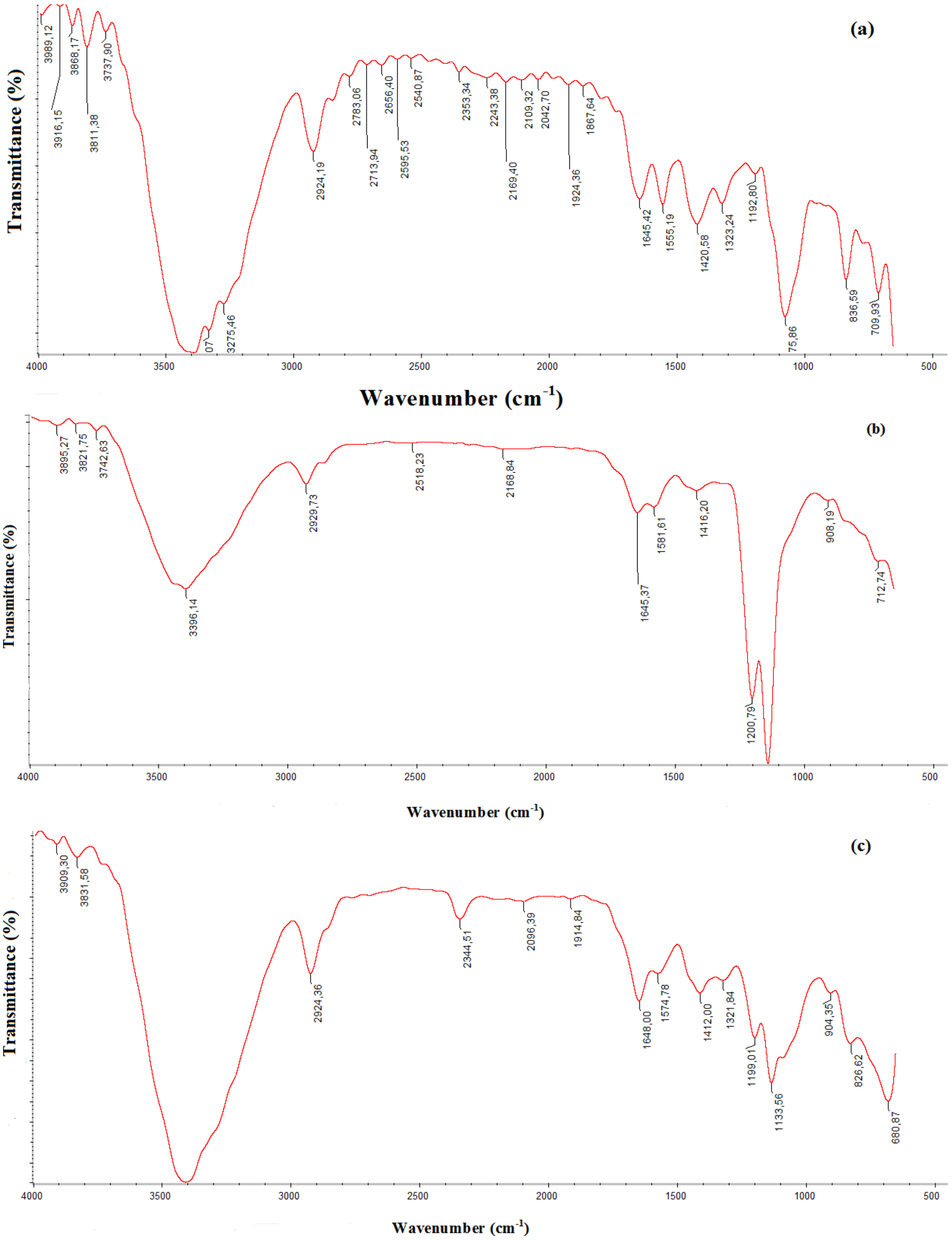

Fig. 6. FT-IR spectra of a) PVA/Mg-Al-LDH; b) PbS/PVA- Mg-Al-LDH nanocomposite film synthesized at 5 cycle; c) PbS/PVA- Mg-Al-LDH nanocomposite film synthesized at 10 cycle.

The infrared bands at 3270–3740 cm^{-1} are attributed to the stretching vibration of OH group. The peak at a higher position corresponds to the free OH group of the starting hydroxide samples. It is the evidence for the presence of LDHin the PVA matrix, O–H bending peaks were observed at 1555 cm^{-1} and 1421 cm^{-1}, and C–H stretching peaks were observed at 2924 cm^{-1} and 2783 cm^{-1} [Figure 6.(a)].These peaks are very intense and broad. This may because both the matrix polyvinyl alcohol and the nanoparticles layered double hydroxide are hydroxyl materials.

The infrared absorption peak at 1134 cm^{-1} was assigned as C–C and C–O-C stretching vibrations [Figure 6.(c)]. This band is recognized as crystallization sensitive band of the PVA matrix [33, 34]. By comparing the infrared spectrum of PbS/PVA-Mg-Al-LDH(5) and PbS/PVA-Mg-Al-LDH(10) it is clear that the spectra mainly exhibit the same features as the PVA/Mg-Al-LDH but the intensity of the peaks was changed, which confirmed the PbS nanoparticles is caped by polyvinyl alcohol.

Table 1. Identification and Assignment of FT-IR bands of PVA/Mg-Al-LDH, PbS/PVA- Mg-Al-LDH (5), and PbS/PVA- Mg-Al-LDH(10).

Assignment	**Band position (cm^{-1})**	
	Literature	**Observed**
O-H	3200-3700, 1420-1330	3333-3740, 1555
H-O-H	1637	1648
C-H	2800-2900, 1465	2924
C-O	1368	absent
C-C	808, 973	836, 908, 828-904
C-O-C	1242, 1159	1199, 1200
S-O	1210, 1062	1200, 1133

4. Conclusion

In this context, we have discussed the synthesis of lead(II)sulfide based nanocomposite on PVA/Mg-Al-LDH composite film by the SILAR method at room temperature. XRD study shows a PbS nanocrystalline structure with the cubic phase. The PVA was used as an organic capping agent to control the growth of the PbS nanocrystal. The average size of PbS nanoparticles were determined 4.08 nm and 1.33 nm for 5 cycle and 10 cycle. The optical absorption study confirmed when the PbS nanoparticles are dispersed in the PVA polymer matrix, they can well fit the interstitial spaces between the polymer chains and thus an increase in the optical conductivity. We observed that the particles are distributed across the polymer composite surface, and the deposited films are composed of regularly shaped crystallites in the SEM images. FT-IR analysis showed that the peak at a higher position corresponds to the free OH group of the starting hydroxide samples and it is the evidence for the presence of LDH in the PVA matrix. The intensity of the peaks was changed, which confirmed the PbS nanoparticles is capped by polyvinyl alcohol.

Khazangul A. Ibrahimova: Conceived and designed the experiments; Performed the experiments; Analyzed and interpreted the data; Wrote the paper. Abdulsaid A. Azizov, Ofeliya O. Balayeva&Rasim M. Alosmanov: Conceived and designed the experiments; Analyzed and interpreted the data, Contributed reagents, materials, analysis data. Reyhan M. Aghayeva& Mirheydar H. Abbasov: Analyzed and interpreted the data.

Acknowledgements

This work was supported by the Baku State University, the department of Polymer Chemistry. The authors thank BSU, NanoResearch Laboratory for the XRD results, and the spectral analyisis group of Institute of Catalysis and Inorganic chemistry of the Azerbaijan National Academy of Sciences for the FTIR results.

References

[1] J. Muñoz-García, L. Vázquez, R. Cuerno, J.A. Sánchez-García, M. Castro and R. Gago, Toward Functional Nanomaterials, Springer US, 2009, 323, 98;

https://doi.org/10.1007/978-0-387-77717-7_10

[2] J.H. Choy, S.Y. Kwak, J.S. Park, and Y.J. Jeong, J Mater.Chem 2001, 11, 1667-71; https://doi.org/10.1039/b008680k

[3] I. Cendoya; L. Lopez; A. Alegria; and C. Mijangos, J. Polym. Sci. 2001, 39, 1968-197; https://doi.org/10.1002/polb.1172

[4] .4 J.C. Ferrer, A.S. Castillo, J.L. Alonso, S.F. de Avila, and R. Mallavia, Mater.Lett.. 2009, 63, 638-640; https://doi.org/10.1016/j.matlet.2008.12.007

[5] J. Yeun, G-S. Bang, B.J. Park; S.K. Ham, and J-H. Chang, J. Appl. Polym. Sci. 2006, 101 , 591-596; https://doi.org/10.1002/app.23372

[6] Q. Wang, X. Zhang, C. J. Wang, J. H. Zhu, Z. H. Guo,and D. O'Hare, J Mater Chem 2012, 22, 19113-21; https://doi.org/10.1039/c2jm33493c

[7] K. Q. Zhou, S. H. Jiang, C. L. Bao, L. Song, B. B. Wang, G. Tang, Y. Hu, and Z. Gui, RSC Adv. 2012, 2, 11695-703; https://doi.org/10.1039/c2ra21719h

[8] H. Karami, M. Ghasemi, and S. Matini, Int. J. Electrochem. Sci. 2013, 8, 11661-11679

[9] OGh Abdullah, D.R. Saber, and S.A. Taha, Adv. Mater. Letters. 2015, 6, 153-157; https://doi.org/10.5185/amlett.2015.5687

[10] H. Wu, Y. Yang, E. Oh, F. La, and D. Yu, Nanotechnology, 2012, 23, 265602; https://doi.org/10.1088/0957-4484/23/26/265602

[11] A.V. Borhade, and B.K. Uphade, Chalcogenide.Lett.2012, 9, 299-306; https://doi.org/10.1155/2012/362680

[12] N. Soltani, E. Saion, M.Z. Hussein, M. Erfani, A. Abedini, G. Bahmanrokh, M. Navasery and P. Vaziri, .Int. J. Mol. Sci. 2012, 13, 12242; https://doi.org/10.3390/ijms131012242

[13] OGh Abdullah, and D.R. Saber, Appl. Mech. Mater.2012, 110, 177-182; https://doi.org/10.4028/www.scientific.net/AMM.110-116.177

[14] C. Shaowei, A. Lindsay, and M. Jennifer, J. Chem. Mater. 2000,12, 3864; https://doi.org/10.1021/cm000653e

[15] K.E. Strawhecker, and E. Manias. Macromolecules. 2001, 34, 8475-8482; https://doi.org/10.1021/ma0101862

[16] P. Scherrer, Nachrichten von der Gesellschaft der Wissenschaftenzu Gottingen and Mathematisch-PhysikalischeKlasse 1918, 20, 98-100.

[17] O.O. Balayeva, A.A. Azizov, M.B. Muradov, A.M. Maharramov, G.M. Eyvazova, R.M. Alosmanov, Z.Q. Mamiyev, and Z.A. Aghamaliyev, Materials Research Bulletin. 2016, 75, 155-161; https://doi.org/10.1016/j.materresbull.2015.11.037

[18] Kh.A.Ibrahimova, A.A. Azizov, O.O. Balayeva, R.M. Alosmanov, and S.C.Mammadyarova.J. Mendeleev Communications.2021, 31 (1), 100-103; https://doi.org/10.1016/j.mencom.2021.01.031

[19] L.-S. Li, J. Hu, W. Yang, and A. P. Alivisatos, Nano Lett. 2001, 1, 349; https://doi.org/10.1021/nl015559r

[20] T. M. Hammad, J.K. Salem, S. Kuhn, N. M. Abu, and Sh,R. Hempelmann, Journal of Luminescence. 2014, 14, 00411-6

[21] Y. Ni, F. Wang, H. Liu, G. Yin, J. Hong, X. Ma, and Z. J. Xu, Cryst. Growth. 2004, 262, 399; https://doi.org/10.1016/j.jcrysgro.2003.10.053

[22] G. Zhou, M. Lu, Z. Xiu, S. Wang, H. Zhang, Y. Zhou, and et.,al. J. Phys.Chem. 2006, 110, 6543-8; https://doi.org/10.1021/jp0549881

[23] A.A. Patel, F. Wu, J.Z. Zhang, C.L. Torres-Martinez, R.K. Mehra, Y. Yang, and S.H. Risbud, J.Phys. Chem. 2000, 104, 11598; https://doi.org/10.1021/jp000639p

[24] Y. Wang and W. Mahler, Opt. Cornrnun. 1987, 61, 233; https://doi.org/10.1016/0030-4018(87)90145-3

[25] L. Deyu, W. Yiying, K. Philip, S. Li, Y. Peidong, and M. Arun, Applied Physics Letters. 2003, 15, 2934 - 2936.

[26] J. Tauc, Amorphous and Liquid Semiconductor (Plenum Publishing Company LTD, London,

1973)
[27] L. Mohapatra, K. Parida, M. Satpathy, J. Phys. Chem.2012, 116, 13063-13070; https://doi.org/10.1021/jp300066g
[28] U. Elfurawi, Phys. Rev. 2012, 92, 1324
[29] B.J. Ramaraj, Appl. Polym.Sci. 2007, 103, 1127- 12; https://doi.org/10.1002/app.24612
[30] Y. Wang, A. Suna, W. Mahler, and R. Kasowski, J. Chem. Phys. 1987, 87, 7315-22; https://doi.org/10.1063/1.453325
[31] K. Nakane, T. Yamachita, K. Iwakura, F. Suzuki, J. Appl. Polym. Sci. 1999, 74, 133; https://doi.org/10.1002/(SICI)1097-4628(19991003)74:1<133::AID-APP16>3.0.CO;2-N
[32] T. Dippong, F. Goga, E-A. Levei and O. Cadar, J Solid State Chem 2019;275, 159-66; https://doi.org/10.1016/j.jssc.2019.04.011
[33] B. Ramaraj, P. Rajalingam, Gangaradhakrishnan. Intl. J. Polym. Mater. 1992, 9, 283
[34] Gyeong-Man Kim, Ashraf ShAsran, Georg H Michler, Paul Simon and JeongSook Kim, Bioinspiration&Biomimetics. 2008, 3, 046003; https://doi.org/10.1088/1748-3182/3/4/046003